



HAL
open science

Halogen and chalcogen-bonding interactions in sulphur-rich π -electron acceptors

Y. Le Gal, A. Colas, F. Barrière, V. Dorcet, T. Roisnel, D. Lorcy

► **To cite this version:**

Y. Le Gal, A. Colas, F. Barrière, V. Dorcet, T. Roisnel, et al.. Halogen and chalcogen-bonding interactions in sulphur-rich π -electron acceptors. *CrystEngComm*, 2019, 21 (12), pp.1934-1939. 10.1039/c8ce02046a . hal-02090018

HAL Id: hal-02090018

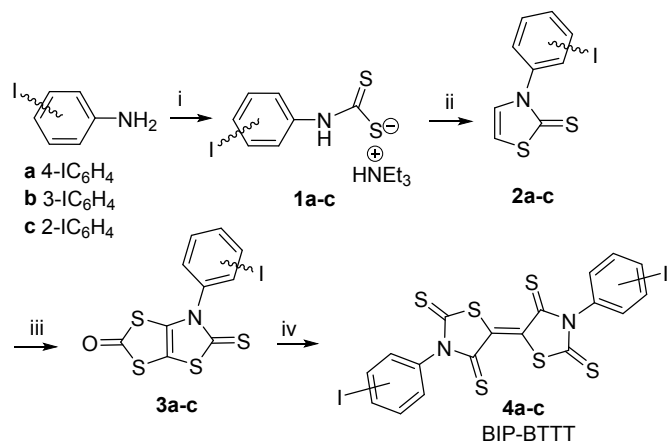
<https://univ-rennes.hal.science/hal-02090018>

Submitted on 17 Apr 2019

HAL is a multi-disciplinary open access archive for the deposit and dissemination of scientific research documents, whether they are published or not. The documents may come from teaching and research institutions in France or abroad, or from public or private research centers.

L'archive ouverte pluridisciplinaire **HAL**, est destinée au dépôt et à la diffusion de documents scientifiques de niveau recherche, publiés ou non, émanant des établissements d'enseignement et de recherche français ou étrangers, des laboratoires publics ou privés.

strategy for the synthesis of the acceptor skeleton.⁹ The acceptors BIP-BTTT **4a-c** were therefore synthesized by simply heating the bicyclic structures **3a-c** into refluxing toluene. These acceptors **4a-c** were obtained as deep purple compounds poorly soluble in common organic solvents, the less soluble one being *para*-substituted **4a**.



Scheme 1. Synthetic path to BIP-BTTT derivatives **4a-c**, 26-36% yield from **2a-c**. Reactants and conditions: i) CS₂, NEt₃; ii) ClCH₂CHO, H₂SO₄; iii) LDA, S₈, (Cl₃CO)₂CO; iv) toluene, Δ.

Electrochemical investigations carried out by cyclic voltammetry allowed us to determine the redox potentials of these derivatives. They were performed in DMSO for the three acceptors **4a-c** and in CH₂Cl₂ for **4b-c**; **4a** being not soluble enough in dichloromethane. The redox potentials are collected in Table 1 together with those of DEBTTT (R = Et, Chart 1) for comparison. Two reversible monoelectronic reduction waves are observed for these three acceptors, either in DMSO or in CH₂Cl₂, attributed to the successive reduction of the acceptor into the radical anion and the dianion. Compared to DEBTTT, in both solvents the redox potentials of the acceptors **4a-c** are slightly shifted towards more anodic potentials indicating a weak effect of the iodophenyl substituent on the overall accepting ability of these molecules. **4a-c** and DEBTTT exhibit slightly lower electron accepting ability than TCNQ (E₁ = 0.18 V and E₂ = -0.37 V vs SCE).¹⁴

Table 1 Redox potentials E_{1/2} V vs SCE, in CH₂Cl₂ and DMSO for DEBTTT and **4a-c**

Acceptors	CH ₂ Cl ₂		DMSO	
	E _{1/2} ¹	E _{1/2} ²	E _{1/2} ¹	E _{1/2} ²
DEBTTT	-0.05	-0.44	0.06	-0.41
4a			0.09	-0.33
4b	-0.01	-0.43	0.1	-0.34
4c	-0.04	-0.48	0.05	-0.37

Crystals of sufficient quality for an X-ray diffraction study were obtained by slow concentration of a CH₂Cl₂ solution of **2b**, **3a** and **3c** as well as from a CHCl₃ solution of the acceptor **4c**. The molecular structure of **2b** is reported in Figure 1. The thiazole core is planar, while the phenyl ring is located in a plane forming a dihedral angle of 63.4(5)° with the thiazoline-2-thione core. The sulphur atoms can behave as a Lewis base and form intermolecular halogen bonding with the iodine atom of a neighbouring molecule.^{13,15} However in **2b**, only a short distance between the hydrogen atom of the thiazoline ring and the sulphur atom of the thione (2.788 (4) Å), assigned to an hydrogen bond (HB), was observed.

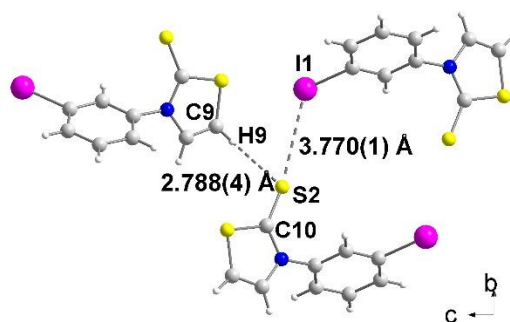


Fig. 1 View of the C-H...S= and C-I...S= interactions on the *bc* plane for **2b**.

Table 2 Relevant interatomic distances (Å) and angles (°) for the halogen bonding, hydrogen bonding and chalcogen interactions. The van der Waals contact distances amount to S...I: 3.78 Å, S...S: 3.60 Å, S...O: 3.32 Å, O...I: 3.50 Å, H...S: 3.00 Å.

	Distances (Å)		Angles (°)	
2b	S ₂ ...H 2.788(4)	C ₉ -H ₉ ...S ₂ 175.9(3)	H ₉ ...S ₂ =C ₁₀ 98.4(2)	
3a	O ₁ ...I ₁ 3.271(12)	C ₈ -I ₁ ...O ₁ 161.4 (4)	I ₁ ...O ₁ =C ₄ 109.2(8)	
	S ₁ ...S ₃ 3.329(4)			
3c	O ₁₂ ...I ₁ 3.252 (5)	C ₁ -I ₁ ...O ₁₂ 154.6 (9)	I ₁ ...O ₁₂ =C ₁₁ 111.1(2)	
	S ₂ ...S ₄ 3.416(1)			
4c	S ₁₅ ...I ₂ 3.763(7)	C ₂₁ -I ₂ ...S ₁₅ 155.5(5)	I ₂ ...S ₁₅ =C ₆₄ 118.7(6)	
	S ₁₆ ...I ₁ 3.390(11)	C ₁ -I ₁ ...S ₁₆ 158.2(3)	I ₁ ...S ₁₆ =C ₆₂ 119.4(6)	
	S ₅ ...I ₁₁ 3.533(4)	C ₅₁ -I ₁₁ ...S ₅ 156.3(3)	C ₁₂ =S ₅ ...I ₁₁ 124.9(5)	
	S ₃ ...S ₆ 3.177(7)			

The molecular structures of dithiol-2-ones **3a** and **3c** are reported in Figure 2. For both derivatives the dithiol-2-one and the fused thiazoline core are coplanar and form with the plane of the aromatic substituent a dihedral angle of 50.5(2)° for **3a** and 100.2(3)° for **3c**. Short I...O contacts are observed between two neighbouring molecules of 3.271 Å for **3a** and 3.252 Å for

3c, corresponding to a reduction ratio of 93.4% and 92.9% respectively, relative to the van der Waals contact distance (3.50 Å), indicating a sizeable XB interaction between neighbouring molecules (Figure 2a and 2b).¹⁶ The C-I...O angles, at 161.4° and 154.6°, are here closer to linearity and consistent with an XB interaction. In addition, for both structures, chalcogen...chalcogen contacts are also observed between neighboring molecules, at a distance shorter than the sum of the van der Waals radii, either of the two sulphur centers (3.60 Å) or the sulphur and the oxygen atoms (3.32 Å). The shortest sulphur...sulphur contacts measured for **3a** and **3c** are reported in Figures 2c and 2d. The crystal structure of **3a** reveals S...O and S...S distances of 3.274(12) Å and 3.329(5) Å respectively, the latter corresponds to 93% of the van der Waals distance and is due to strong non covalent bonding between two molecules. Comparatively the S...S distances within **3c** (the shortest being 3.416(1) Å) are longer than in **3a**. This is ascribed to a steric effect in the solid state of the *ortho* position of the iodine atom on the phenyl ring.

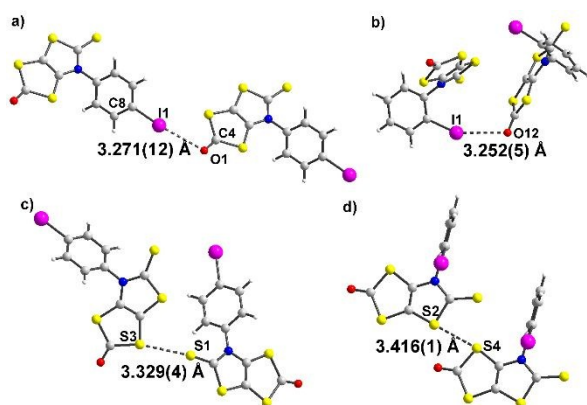


Fig. 2 View of the XB interactions, O...I contacts shorter than the sum of the van der Waals radii in dark grey dotted lines in **3a** (a) and **3c** (b). View of the chalcogen interactions, S...S contacts shorter than the sum of the van der Waals radii in dark grey dotted lines in **3a** (c) and **3c** (d).

Among the three electron acceptors, only the *ortho* substituted derivative **4c** could be analysed by X-ray diffraction study. The molecular structure of this derivative is presented in Figure 3. It crystallizes in the triclinic system, space group P-1, with two crystallographically independent molecules in the unit cell in general position. This acceptor exhibits a planar skeleton and a *trans* configuration of the two thiazoline-2-thione rings with short intramolecular S...S contacts between the S atom of a thiocarbonyl group and the S atom of the thiazole ring (2.94 Å/2.91 Å). These short S...S contacts are in the same range as those observed for different acceptors belonging to the same family.⁹

Interestingly, the *ortho*-iodophenyl substituents on the nitrogen atoms have a similar orientation with the iodine

pointing in the same direction above the plane of the acceptor. The plane of the phenyl rings is almost perpendicular to the plane of the acceptor. The molecules are associated through I...S=C XB interaction networks between I₁...S₁₆ 3.390(11) Å and I₁₁...S₅ 3.533(11) Å for the most significant short distances corresponding respectively to 89.7% and 93.4% of the van der Waals distances. Besides these intramolecular contacts, short S...S intermolecular contacts are also observed between neighbouring molecules, S₃...S₆ 3.177(7) Å lower than the van der Waals radius of sulphur, corresponding to a reduction ratio of 88.2%. Nevertheless, due to steric hindrance generated by the iodophenyl rings, these S...S contacts within these acceptors are less numerous than those observed with DEBTTT where extensive three-dimensional S...S interactions were noticed.⁹

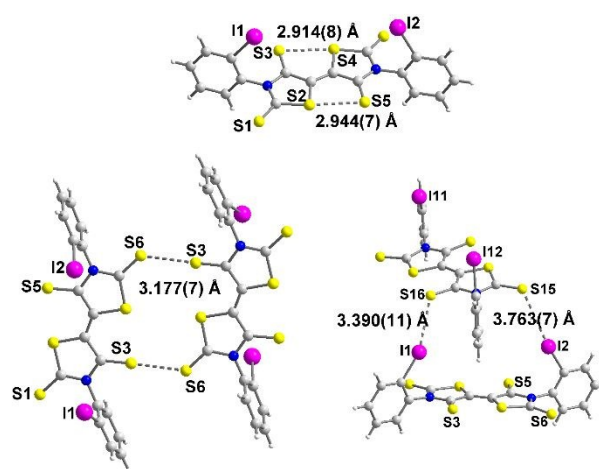


Fig. 3 Molecular structure of the acceptor **4c** showing the intramolecular S...S contacts (top), the shortest intermolecular contacts (bottom left) and the XB bonds between two neighbouring molecules (bottom right).

Electrostatic surface potential calculations have been performed on the optimized geometry of the four molecules that have been crystallographically characterized, namely **2b**, **3a**, **3c** and **4c**. These calculations were carried out in order to estimate the halogen bond donor abilities of the iodophenyl substituent within these different structures and to rationalize the interactions taking place in the crystal.⁹ As shown in Figure 4, for **2b** the maximum calculated positive electrostatic surface potential (ESP) is found at the hydrogen atoms located on the thiazole ring (+31.74 kcal.mol⁻¹) compared to only +23.89 kcal.mol⁻¹ at the iodine atom. The most negative calculated ESP is -29.09 kcal.mol⁻¹ and located on the thione's sulphur atom (C=S). This calculated charge repartition is in good agreement with the organization of the molecule **2b** in the solid state where predominant hydrogen bonding interactions were observed between the hydrogen atom on the thiazole ring and the sulphur atom of the thione, while no specific halogen bonding interaction involving the iodine atom was detected.

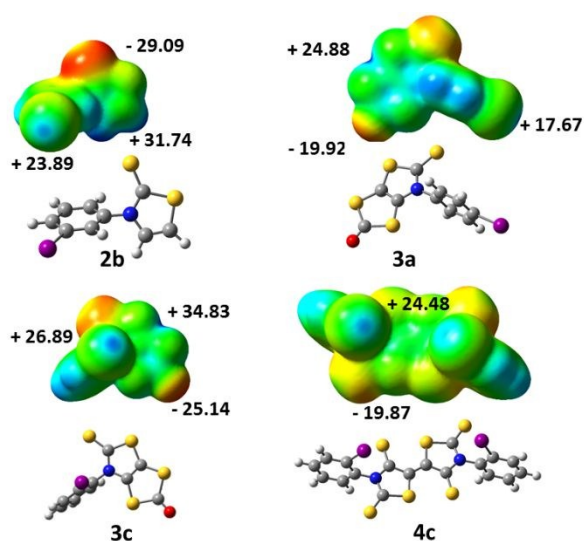


Fig. 4 Molecular electrostatic potential surface mapped at the $0.001 \text{ e} \cdot \text{au}^{-3}$ isodensity surface for **2b**, **3a**, **3c** and **4c**. The common colour scale ranges from $-29 \text{ kcal} \cdot \text{mol}^{-1}$ (red) to $+35 \text{ kcal} \cdot \text{mol}^{-1}$ (blue).

For the dithiol-2-one **3a** and **3c**, the most negative calculated ESP is now located on the oxygen atom of the dithiole rings ($\text{C}=\text{O}$, -19.92 and $-25.14 \text{ kcal} \cdot \text{mol}^{-1}$ respectively) while the most positive ESP is on the bicyclic structure ($+24.88$ and $+34.83 \text{ kcal} \cdot \text{mol}^{-1}$). The electrostatic surface potential value on the σ -hole of the halogen is lower (blue dot on the iodine atom in Figure 5, $+17.67$ and $+26.89 \text{ kcal} \cdot \text{mol}^{-1}$). Despite these slightly lower values, the organization of both molecules in the solid state shows XB interactions ($\text{C}=\text{O} \cdots \text{I}$) between their iodine atom and the oxygen atom of a vicinal molecule.

The acceptor **4c** is the only example where the highest ESP value over the whole molecule is found at the σ -hole of the iodine atom ($+24.48 \text{ kcal} \cdot \text{mol}^{-1}$, Figure 5) while for the three other derivatives, it was either found on an hydrogen atom for **2b** or on the bicycle structure for **3**. The most negative calculated ESP for **4c** is found on the sulphur atoms of the thione ($-19.96 \text{ kcal} \cdot \text{mol}^{-1}$). In accordance with these calculations, the iodine atom of this acceptor is indeed involved in short XB interactions with the thione's sulphur atom in the solid state (Table 2).

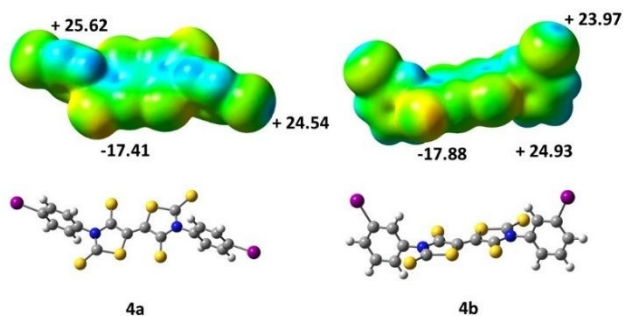


Fig. 5 Molecular electrostatic potential surface mapped at the $0.001 \text{ e} \cdot \text{au}^{-3}$ isodensity surface for **4a** and **4b**. The colour scales range from $-29 \text{ kcal} \cdot \text{mol}^{-1}$ (red) to $+35 \text{ kcal} \cdot \text{mol}^{-1}$ (blue).

We also performed some ESP calculations for the two other acceptors that have not been crystallographically characterized in order to analyse the influence of the localization of the halogen atom. For both acceptors, **4a** and **4b**, the most negative calculated ESP is located on the thione's sulphur atom ($\text{C}=\text{S}$) as for the acceptor **4c**. On the other hand, the highest ESP value over the whole molecules **4a** and **4b** is not found at the σ -hole like for **4c** (Figure 5) but located para to the iodine atom on the aromatic ring, potentially a less favorable charge distribution for the growing of crystals in these cases.

Conclusions

In this study we investigated the synthesis of sulphur-rich electron π -acceptors, the bithiazolidinylidenes, substituted by iodophenyl substituents, which can act as halogen bond donor toward thione ($\text{C}=\text{S}$) or ketone ($\text{C}=\text{O}$) groups acting as XB acceptors. Single crystals of the synthetic intermediates as well as one of the acceptors have been obtained. For the precursors, when the thione ($\text{C}=\text{S}$) and ketone ($\text{C}=\text{O}$) groups are present on the molecule, a halogen bond is formed between the iodine atom of one molecule and the $\text{C}=\text{S}/\text{C}=\text{O}$ moieties of the neighbouring ones. For the acceptor **4c**, in accordance with the calculated ESP maxima, $\text{I} \cdots \text{S}=\text{C}$ halogen bonds are observed between neighbouring molecules as well as $\text{S} \cdots \text{S}$ interactions. Thus we managed to generate from these BIPBTTT acceptors the coexistence of two types of intermolecular interactions in the solid state. The next step will be the design of sulphur-rich electron acceptor substituted by groups bearing an iodine atom but less bulky than phenyl in order to increase the strength of the intermolecular interactions.

Experimental section

All commercial chemicals were used without further purification. The solvents were purified and dried by standard methods. All the NMR spectra were obtained in CDCl_3 unless indicated otherwise. Chemical shifts are reported in ppm and ^1H NMR spectra were referenced to residual CHCl_3 (7.26 ppm) and ^{13}C NMR spectra were referenced to CHCl_3 (77.2 ppm). The ^{13}C NMR spectra of the acceptors **4a-c** could not be obtained due to their low solubility. Melting points were measured on a Kofler hot-stage apparatus and are uncorrected. Mass spectra and Elemental analyses were performed at the Centre Régional de Mesures Physiques de l'Ouest, Rennes. Cyclic voltammetry were carried out on a 10^{-3} M solution in CH_2Cl_2 , containing 0.1 M $n\text{Bu}_4\text{NPF}_6$ as supporting electrolyte. Voltammograms were recorded at 0.1 Vs^{-1} on a platinum electrode and the potentials were measured versus the Saturated Calomel Electrode (SCE).

N-iodophenyl-1,3-thiazoline-2-thione 2a-c : To a solution of 4-iodoaniline, 3-iodoaniline or 2-iodoaniline (12 g, 54.8 mmol) was added 100 mL of triethylamine and 100 mL of carbon disulphide. The solution was stirred under argon 24h. The solution was filtered and

the yellow solid was washed with diethylether. The dithiocarbamate salts **1a-c** were used without further purification; **1a**: yield: 95%, Mp : 92°C. ¹H NMR (300 MHz) δ 1.30 (t, 9H, ³J=7.3Hz, CH₃), 3.17 (q, 6H, ³J=7.3Hz, CH₂), 7.43 (m, 2H, Ar), 7.53 (m, 2H, Ar), 9.45 (s, 1H, NH); ¹³C NMR (75 MHz) δ 8.8 (CH₃), 46.0 (CH₂), 88.2 (Ar), 125.2 (Ar), 137.7 (Ar), 140.8 (Ar), 214.3 (C=S); **1b**: yield: 97%; Mp: 100°C; ¹H NMR (300 MHz) δ 1.36 (t, 9H, ³J=7.3Hz, CH₃), 3.23 (q, 6H, ³J=7.3Hz, CH₂), 6.99 (t, 1H, ³J=8.1Hz, Ar), 7.39 (d, 1H, ³J=8.1Hz, Ar), 7.62 (d, 1H, ³J=8.1Hz, Ar), 8.10 (s, 1H, Ar), 9.40 (s, 1H, NH); ¹³C NMR (75 MHz) δ 8.8 (CH₃), 46.0 (CH₂), 93.3 (Ar), 122.8 (Ar), 129.7 (Ar), 131.8(Ar), 133.3 (Ar), 142.1 (Ar), 214.7 (C=S); **1c**: yield : 92%; Mp: 95 °C; ¹H NMR (300 MHz) δ 1.36 (t, 9H, ³J=7.3Hz, CH₃), 3.22 (q, 6H, ³J=7.3Hz, CH₂), 6.85 (m, 1H, Ar), 7.31 (m, 1H, Ar), 7.78 (d, 1H, ³J=8.1Hz, Ar), 8.08 (d, 1H, ³J=8.1Hz, Ar), 9.02 (s, 1H, NH); ¹³C NMR (75 MHz) δ 9.2 (CH₃); 46.0 (CH₂); 95.0 (Ar); 114.8 (Ar); 127.7 (Ar); 128.8 (Ar); 138.8 (Ar); 142.2 (Ar); 215.5 (C=S); To a solution of the dithiocarbamate salt (**1a-c**) (20.6 g, 52.0 mmol) was added 1 equivalent of chloroacetaldehyde (0.96 mL, 52.0 mmol). The solution was stirred for 12h at rt and 9/10 of the solvent was evaporated *in vacuo*. The mixture was added to 15 mL of H₂SO₄ at 0°C and stirred for further 10 minutes. The solution was extracted with CH₂Cl₂ (3 x 50 mL), washed with water (3 x 20 mL) and dried over MgSO₄. The precipitate was washed with ethanol. Brown powders were obtained.

2a: yield: 71%; Mp = 211°C; ¹H NMR (300 MHz) δ 6.67 (d, 1H, ³J=4.7Hz, SCH), 7.08 (d, 1H, ³J=4.7Hz, NCH), 7.27 (d, 2H, ³J=4.7Hz, Ar), 7.85 (d, 2H, ³J=4.7Hz, Ar); ¹³C NMR (75 MHz) 95.0 (Ar), 111.6 (C=C), 128.4 (2Ar), 132.1 (C=C), 138.3 (Ar), 138.9 (2Ar), 214.5 (C=S); HRMS (ESI) calcd for C₉H₆INNaS₂ [M+Na]⁺: 341.88786. Found: 341.8882; Anal calcd for C₉H₆INS₂: C, 33.87; H, 1.89; N, 4.39. Found: C, 33.68; H, 1.82; N, 4.38.

2b: yield 87%; Mp : 119°C; ¹H NMR (300 MHz) δ 6.68 (d, 1H, ³J=4.7Hz, SCH), 7.10 (d, 1H, ³J=4.7Hz, NCH), 7.24 (m, 1H, Ar), 7.51 (m, 1H, Ar), 7.80 (m, 2H, Ar), 7.83; ¹³C NMR (75 MHz) δ 93.9 (Ar), 111.6 (C=C), 126.1 (C=C), 130.8 (Ar), 132.1 (Ar), 135.3 (Ar), 138.3 (Ar), 139.3 (Ar), 188.7 (C=S); HRMS (ESI) calcd for C₉H₆INNaS₂ [M+Na]⁺: 341.88786. Found: 341.8881. Anal calcd for C₉H₆INS₂: C, 33.87; H, 1.89; N, 4.39. Found C, 33.51; H, 1.69; N, 4.42.

2c: yield 72%; Mp :180°C; ¹H NMR (300 MHz) δ 6.71 (d, 1H, ³J=4.7Hz, SCH), 6.98 (d, 1H, ³J=4.7Hz, NCH), 7.22 (m, 1H, Ar), 7.40 (m, 1H, Ar), 7.52 (m, 1H, Ar), 7.99 (m, 1H, Ar); ¹³C NMR (75 MHz) δ 96.7 (Ar), 111.7 (C=C), 129.2 (C=C), 129.8 (Ar), 131.4 (2Ar), 140.4 (Ar), 141.5 (Ar), 189.0 (C=S); HRMS (ESI) calcd for C₉H₆INNaS₂ [M+Na]⁺: 341.88786. Found 341.8877. Anal calcd for C₉H₆INS₂: C, 33.87; H, 1.89; N, 4.39. Found: C, 33.76; H, 1.69; N, 4.44.

Synthesis of bicycle 3a-c: To a -10°C cooled solution of thiazoline (**2a-c**) (1 g, 3.12 mmol) in 80 mL of dry THF under nitrogen was added a solution of LDA prepared from diisopropylamine (0.66 ml, 4.8 mmol) and *n*-BuLi 1.6M (2.93 mL, 4.8 mmol) in 10mL of dry THF. After stirring for 30 min at -10°C, sulphur S₈ (150 mg, 4.8 mmol) was added and the solution was stirred for an additional 30 min. A solution of LDA diisopropylamine (0.88mL, 6.24 mmol) and *n*-BuLi (3.9 mL, 6.24 mmol) in 15mL of dry THF was added. The mixture was stirred for 3 hours and S₈ (200 mg, 6.24 mmol) was added. After 30 min, triphosgene (1.11 g, 3.7 mmol) was added to the reaction mixture. The reaction was stirred overnight and water (15 mL) was slowly added. The solvent was evaporated *in vacuo*. Dichloromethane (50

mL) was added and the solution was washed with water (3 x 20 mL) and dried over MgSO₄. The concentrated solution was purified by chromatography on silica gel using CH₂Cl₂-petroleum ether as the eluent. Brown powders were obtained for **3a** and **3c**. **3b** was not isolated, the crude oil was used without further purification.

3a : yield : 36%; Mp = 174°C; ¹H NMR (300 MHz) δ 7.20 (m, 2H, Ar) ; 7.92 (m, 2H, Ar). ¹³C NMR (CDCl₃, 75 MHz) δ = 96.8 (Ar), 102.1 (C=C), 127.1 (C=C), 128.3 (2Ar), 137.2 (Ar), 139.6 (2Ar), 186.1 (C=S), 188.1 (C=O); IR $\nu_{(C=S)}$: 1261 cm⁻¹, $\nu_{(C=O)}$: 1695 cm⁻¹; HRMS (ESI) calcd for C₁₀H₄INOS₄ [M+H]⁺: 409.82933. Found: 409.8296; Anal. calcd for C₁₀H₄INOS₄: C, 29.34; H, 0.99; N, 3.42. Found: C, 29.68; H, 1.06; N, 3.50.

3c : yield : 60% ; Mp = 200 °C ; ¹H NMR (300 MHz) δ 7.29 (m, 1H, Ar), 7.44 (m, 1H, Ar), 7.58 (m, 1H, Ar), 8.02 (m, 1H, Ar); ¹³C NMR (75 MHz) δ 94.2 (Ar), 108.1 (C=C), 112.6 (C=C), 131.1 (Ar), 131.7 (Ar), 138.8 (Ar), 139.4 (Ar), 143.7 (Ar), 191.6 (C=S), 192.1 (C=O); IR $\nu_{(C=S)}$: 1289 nm , IR $\nu_{(C=O)}$: 1660 nm; HRMS (ESI) calcd for C₁₀H₄INOS₄ [M+H]⁺: 431.81127. Found: 431.8110; Anal. calcd for C₁₀H₄INOS₄: C, 29.34; H, 0.99; N, 3.42 .Found: C, 29.65; H, 0.92; N, 3.21.

Synthesis of BIP-BTTT 4a-c. A solution of thiazoline-thione **3a-c** (243mg, 0.59 mmol), (crude compound for **3b**) in 30 mL of toluene was refluxed for 16h. 80% of the solvent was removed *in vacuo* and the concentrated solution was filtrated and the precipitate was washed with ethanol. Dark purple powders were obtained. Crystals of **4c** of sufficient quality for X-ray diffraction were obtained by slow evaporation of CHCl₃ solution.

4a: yield: 72%, Mp>250°C; ¹H NMR (CS₂, 300 MHz) δ 7.08 (d, 4H, Ar), 7.89 (d, 4H, Ar); HRMS (ESI) calcd for C₁₈H₉N₂S₆ [M]⁺: 697.70958. Found 697.7101; UV-vis (CHCl₂) $\lambda_{max}(nm)$ (ϵ [L.mol⁻¹.cm⁻¹])= 242 (24640), 358 (11500), 520 (2550); Anal. calcd for [C₁₈H₈l₂N₂S₆ + Toluene (8/1)]: C, 31.93 ; H, 1.28 ; N, 3.95. Found: C, 32.08 ; H, 1.27 ; N, 3.95.

4b: yield : 30% (calculated from **2b**), mp>250°C; ¹H NMR (CS₂, 300 MHz) δ 7.18 (m, 2H, Ar), 7.32(m, 2H, Ar), 7.52 (m, 2H, Ar), 7.83 (m, 2H, Ar); UV-vis (CHCl₂) $\lambda_{max}(nm)$ (ϵ [L.mol⁻¹.cm⁻¹])= 232(36060), 359 (18370), 512(3420); HRMS (ESI) calcd for C₁₈H₉N₂S₆ [M+Na]⁺: 720.69935. Found 720.6993. Analysis calcd for [C₁₈H₈l₂N₂S₆ + Toluene (8/1)]: C, 31.93 ; H, 1.28 ; N, 3.95. Found: C, 32.04 ; H, 1.32 ; N, 4.18.

4c: yield : 60%, mp = 200°C. ¹H NMR (300 MHz) δ 7.27 (m, 2H, Ar), 7.41 (m, 2H, Ar), 7.54 (m, 2H, Ar), 8.02 (m, 2H, Ar); UV-vis (CHCl₂) $\lambda_{max}(nm)$ (ϵ [L.mol⁻¹.cm⁻¹]):226(28670), 358(14928), 511(2270); HRMS (ESI) calcd for C₁₈H₉N₂S₆ [M]⁺ : 697.71068. Found: 697.7107; Analysis calcd for [C₁₈H₈l₂N₂S₆ + Toluene (8/1)]: C, 31.93 ; H, 1.28 ; N, 3.95. Found: C, 31.77 ; H, 1.25 ; N, 3.96.

Crystallography

Data were collected on a D8 VENTURE Bruker AXS diffractometer with graphite-monochromated Mo-K α radiation (λ = 0.71073 Å) for **2b**, **3a**, **3c** and **4c** The structures were solved by dual-space algorithm using the *SHELXT* program,¹⁷ and then refined with full-matrix least-square methods based on *F*² (*SHELXL*).¹⁸ All non-hydrogen atoms were refined with anisotropic atomic displacement parameters. H atoms were finally included in their calculated positions. Concerning

3a, the use of Platon/TwinRotMat¹⁹ routine allowed to detect the presence of a twinning in the measured crystal. Satisfactory final structural refinement has been performed considering the presence of such a twinning and on the hklf5 file format, leading to a refined twin ratio of 0.19. Crystallographic data on X-ray data collection and structure refinements are given in Table 3

Table 3 Crystallographic data

Compound	2b	3a	3c	4c
Formula	C ₉ H ₆ IN ₂ S ₂	C ₁₀ H ₄ INOS ₄	C ₁₀ H ₄ INOS 4	C ₁₈ H ₈ I ₂ N ₂ S ₆
FW (g·mol ⁻¹)	319.17	409.28	409.28	698.42
Crystal system	monoclinic	monoclinic	monoclinic	triclinic
Space group	<i>C</i> 2/ <i>c</i>	<i>P</i> 2 ₁ / <i>n</i>	<i>P</i> 2 ₁ / <i>c</i>	<i>P</i> -1
<i>a</i> (Å)	8.7777(10)	4.1078(7)	8.1394(7)	12.5260(18)
<i>b</i> (Å)	11.1568(15)	24.675(5)	6.9798(7)	14.352(2)
<i>c</i> (Å)	21.241(3)	13.943(3)	22.487(2)	14.522(2)
α (°)	90	90	90	117.141(4)
β (°)	96.632(4)	118.785(7)	94.788(3)	95.478(5)
γ (°)	90	90	90	100.638(5)
<i>V</i> (Å ³)	2066.3(5)	1238.6(4)	1273.1(2)	2234.7(6)
<i>T</i> (K)	150(2)	150(2)	150(2)	150(2)
<i>Z</i>	8	4	4	4
<i>D</i> _{calc} (g·cm ⁻³)	2.052	2.195	2.135	2.076
μ (mm ⁻¹)	3.454	3.238	3.151	3.384
Total refls.	8223	11687	14751	51086
Abs. Corr.	multi-scan	multi-scan	multi-scan	multi-scan
Uniq. refls.	2344	-	2904	10225
(<i>R</i> _{int})	(0.0274)		(0.0404)	(0.1050)
Uniq. refls. (<i>I</i> > 2 σ (<i>I</i>))	2188	8472	2675	6098
<i>R</i> ₁ , <i>wR</i> ₂	0.0307, 0.0974	0.0758, 0.1622	0.0306, 0.0814	0.1160, 0.3164
<i>R</i> ₁ , <i>wR</i> ₂ (all data)	0.0336, 0.1095	0.1094, 0.1758	0.0337, 0.0834	0.1793, 0.3626
GoF	1.101	1.042	1.054	1.079

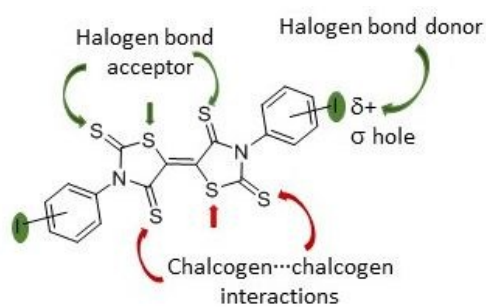
Theoretical Modeling

Electrostatic Surface Potential calculations were carried out on the optimized geometry of the molecules (with Density Functional Theory using the Gaussian 09 Revision D.01 software, the B3LYP functional and the 6-31+G** basis set for all atoms and the LANLdp basis set for iodine). GaussView 5.0.9 was used to generate the figures.

Notes and references

- 1 S. Sutton, C. Risko and J. L. Brédas, *Chem. Mater.*, 2016, **28**, 3-16.
- 2 G. R. Desiraju, *J. Am. Chem. Soc.*, 2013, **135**, 9952-9967.
- 3 R. Gleiter, G. Haberhauer, D. B. Werz, F. Rominger and C. Bleiholder, *Chem. Rev.*, 2018, **118**, 2010-2041.
- 4 G. R. Desiraju, *Cryst. Growth Des.*, 2011, **11**, 896-898.

- 5 E. D. Głowacki, M. Irimia-Vladu, S. Bauer and N. S. Sariciftci, *J. Mater. Chem. B*, 2013, **1**, 3742-3753.
- 6 K. S. Kim, P. Tarakeshwar and J. Y. Lee, *Chem. Rev.*, 2000, **100**, 4145-4185.
- 7 (a) G. Cavallo, P. Metrangolo, R. Milani, T. Pilati, A. Priimagi, G. Resnati and G. Terraneo, *Chem. Rev.*, 2016, **116**, 2478-2601. (b) L. C. Gilday, S. W. Robinson, T. A. Barendt, M. J. Langton, B. R. Mullaney and P. D. Beer, *Chem. Rev.*, 2015, **115**, 7118-7195. (a) G. Cavallo, P. Metrangolo, R. Milani, T. Pilati, A. Priimagi, G. Resnati and G. Terraneo, *Chem. Rev.*, 2016, **116**, 2478-2601. (b) L. C. Gilday, S. W. Robinson, T. A. Barendt, M. J. Langton, B. R. Mullaney and P. D. Beer, *Chem. Rev.*, 2015, **115**, 7118-7195.
- 8 A. S. Mahadevi and G. N. Sastry, *Chem. Rev.*, 2016, **116**, 2775-2825
- 9 (a) Y. Le Gal, N. Bellec, F. Barrière, R. Clérac, M. Fourmigué, V. Dorcet, T. Roisnel, and D. Lorcy, *Dalton Trans.*, 2013, **42**, 16672-16679. (b) Y. Le Gal, D. Ameline, N. Bellec, A. Vacher, T. Roisnel, V. Dorcet, O. Jeannin and D. Lorcy, *Org. Biomol. Chem.*, 2015, **13**, 8479-8486. (c) Y. Le Gal, M. Rajkumar, A. Vacher, V. Dorcet, T. Roisnel, M. Fourmigué, F. Barrière, T. Guizouarn and D. Lorcy, *CrysEngComm*, 2016, **18**, 3925-3933.
- 10 A. Filatre-Furcate, T. Higashino, D. Lorcy and T. Mori, *J. Mater. Chem. C*, 2015, **3**, 3569-3573.
- 11 (a) K. Iijima, Y. Le Gal, T. Higashino, D. Lorcy, T. Mori, *J. Mater. Chem. C*, 2017, **5**, 9121-9127. (b) K. Iijima, Y. Le Gal, D. Lorcy and T. Mori, *RSC Adv.*, 2018, **8**, 18400-18405.
- 12 C. Wang, H. Dong, W. Hu, Y. Liu and D. Zhu, *Chem. Rev.*, 2012, **112**, 2208-2267.
- 13 Y. Le Gal, D. Lorcy, O. Jeannin, F. Barrière, V. Dorcet, J. Lieffrig and M. Fourmigué, *CrystEngComm.*, 2016, **18**, 5474-5481.
- 14 M. L. Kaplan, R. C. Haddon, F. B. Bramwell, F. Wudl, J. H. Marshall, D. O. Cowan and S. Gronowitz, *J. Phys. Chem.*, 1980, **84**, 427-431.
- 15 M. Arca, M. C. Aragoni, F. A. Devillanova, A. Garau, F. Isaia, V. Lippolis, A. Mancini and G. Verani, *Bioinorg. Chem. Appl.*, 2006, 58937.
- 16 P. Auffinger, F. A. Hays, E. Westhof and P. S. Ho, *Proc. Natl. Acad. Sci. USA*, 2004, **101**, 16789-16794.
- 17 G. M. Sheldrick, *Acta Cryst.*, 2015, **A71**, 3-8.
- 18 G. M. Sheldrick, *Acta Cryst.*, 2015, **C71**, 3-8.
- 19 A. L. Spek, *Acta Cryst.*, 1990, **A46**, C34.

Graphical abstract

Sulphur and iodine heteroatoms on the acceptor skeleton induce chalcogen... chalcogen and halogen-bonding interactions.